



UvA-DARE (Digital Academic Repository)

Optimization of adaptive radiation therapy in cervical cancer: Solutions for photon and proton therapy

van de Schoot, A.J.A.J.

Publication date

2016

Document Version

Final published version

[Link to publication](#)

Citation for published version (APA):

van de Schoot, A. J. A. J. (2016). *Optimization of adaptive radiation therapy in cervical cancer: Solutions for photon and proton therapy*. [Thesis, fully internal, Universiteit van Amsterdam].

General rights

It is not permitted to download or to forward/distribute the text or part of it without the consent of the author(s) and/or copyright holder(s), other than for strictly personal, individual use, unless the work is under an open content license (like Creative Commons).

Disclaimer/Complaints regulations

If you believe that digital publication of certain material infringes any of your rights or (privacy) interests, please let the Library know, stating your reasons. In case of a legitimate complaint, the Library will make the material inaccessible and/or remove it from the website. Please Ask the Library: <https://uba.uva.nl/en/contact>, or a letter to: Library of the University of Amsterdam, Secretariat, P.O. Box 19185, 1000 GD Amsterdam, The Netherlands. You will be contacted as soon as possible.

Chapter 4

Beam configuration selection for robust intensity-modulated proton therapy in cervical cancer using Pareto front comparison

A version of this chapter has been published as:

Beam configuration selection for robust intensity-modulated proton therapy in cervical cancer using Pareto front comparison

A.J.A.J. van de Schoot, J. Visser, Z. van Kesteren, T.M. Janssen, C.R.N. Rasch and A. Bel

Physics in Medicine and Biology 2016; 61(4): 1780–1794.

<http://dx.doi.org/10.1088/0031-9155/61/4/1780>

Abstract

Purpose

The Pareto front reflects the optimal trade-offs between conflicting objectives and can be used to quantify the effect of different beam configurations on plan robustness and dose-volume histogram parameters. Therefore, our aim was to develop and implement a method to automatically approach the Pareto front in robust intensity-modulated proton therapy (IMPT) planning. Additionally, clinically relevant Pareto fronts based on different beam configurations will be derived and compared to enable beam configuration selection in cervical cancer proton therapy.

Material & Methods

A method to iteratively approach the Pareto front by automatically generating robustly optimized IMPT plans was developed. To verify plan quality, IMPT plans were evaluated on robustness by simulating range and position errors and recalculating the dose. For five retrospectively selected cervical cancer patients, this method was applied for IMPT plans with three different beam configurations using two, three and four beams. Three-dimensional Pareto fronts were optimized on target coverage (CTV $D_{99\%}$) and OAR doses (rectum $V_{30\text{Gy}}$; bladder $V_{40\text{Gy}}$). Per patient, proportions of non-approved IMPT plans were determined and differences between patient-specific Pareto fronts were quantified in terms of CTV $D_{99\%}$, rectum $V_{30\text{Gy}}$ and bladder $V_{40\text{Gy}}$ to perform beam configuration selection.

Results

Per patient and beam configuration, Pareto fronts were successfully sampled based on 200 IMPT plans of which on average 29% were non-approved plans. In all patients, IMPT plans based on the 2-beam set-up were completely dominated by plans with the 3-beam and 4-beam configuration. Compared to the 3-beam set-up, the 4-beam set-up increased the median CTV $D_{99\%}$ on average by 0.2 Gy and decreased the median rectum $V_{30\text{Gy}}$ and median bladder $V_{40\text{Gy}}$ on average by 3.6% and 1.3%, respectively.

Conclusion

This study demonstrates a method to automatically derive Pareto fronts in robust IMPT planning. For all patients, the defined four-beam configuration was found optimal in terms of plan robustness, target coverage and OAR sparing.

4.1 | Introduction

The primary treatment for patients with locally advanced uterine cervical cancer consists of photon-based external-beam radiation therapy (RT) with concurrent chemotherapy or hyperthermia [18,72], often followed by brachytherapy [118]. The introduction of intensity-modulated RT (IMRT), which enables highly conformal target doses with steep dose fall-offs, decreased organ at risk (OAR) doses [119,120], but also required adequate patient set-up using image guidance in order to fully exploit the potential advantage. Besides the reduction of positioning errors and the quantification of geometric uncertainties induced by interfraction anatomical changes of pelvic organs [89,92], image-guided RT (IGRT) including daily soft-tissue visualization offers possibilities for online adaptive RT. Moreover, the implementation of rotational IMRT techniques further improved OAR sparing with the addition of decreased treatment delivery time [32]. Despite all improvements, healthy surrounding tissue still receives a substantial amount of dose which causes serious toxicity and significantly reduces quality of life [121].

Because of its characteristic Bragg peak, protons have certain distinct advantages over conventionally used X-rays. Among others, uterine cervical cancer patients may also benefit from proton therapy (PT) and interest in the application of PT has increased recently [24,70,71,122]. Intensity-modulated PT (IMPT) using pencil beam scanning technology paints dose to target volumes while minimizing surrounding dose, enabling adequate dose delivery to complex-shaped target volumes and limited OAR doses. However, proton-based RT is sensitive to range and position uncertainties and therefore IMPT plan robustness is necessary to guarantee target coverage and OAR sparing.

Although several studies investigated PT for uterine cervical cancer patients [70,71,123,124], none of them used treatment plans that are robust against possible position and range uncertainties. Besides the lack of plan robustness, no agreement between beam configurations was observed and the effect of beam configurations on dose-volume histogram (DVH) parameters was not considered. Therefore, the optimal beam configuration and the influence of uncertainties on dose distributions in cervical cancer PT are still unknown. In order to obtain patient-specific optimal dose distributions in addition to robustness, the number of beams and associated gantry angles should be included in the process of optimization. Although some studies demonstrated gantry angle optimization algorithms in photon-based RT [125-127], complete beam configuration optimization is currently not implemented in the process of plan optimization.

To objectively investigate the use of different beam configurations in IMPT planning without the arbitrariness of individual planning decisions, the set of Pareto optimal plans that reflects the optimal trade-offs between conflicting objectives (i.e. the Pareto front) are compared. The feasibility of using Pareto fronts as an evaluative and comparative tool has been shown [128]. Along these lines, we aim to investigate the influence of beam configuration on plan robustness and DVH parameters by comparing Pareto fronts obtained with various sets of gantry angles. The purpose of this study was therefore to develop and implement a method to derive the Pareto front based

on robust IMPT planning to be used in clinical practice. In addition, Pareto fronts with a potential clinical relevance derived using different beam configurations will be compared to enable beam configuration selection for cervical cancer PT.

4.2 | Material & Methods

Patient data

Data of five patients with a cervical carcinoma and treated with photon-based RT were included retrospectively. These patients were treated in prone treatment position using a belly board device for bowel dose minimization [26]. CT images (LightSpeed RT16 system, General Electric Company, Waukesha WI, USA) with a slice thickness of 2.5 mm acquired for photon-based RT treatment planning were also used for IMPT treatment planning. Relevant regions of interest for IMPT treatment planning include the delineated OARs (body, rectum, bladder and bowel cavity) and the clinical target volume (CTV), encompassing the cervix, gross tumor volume (GTV), corpus uterus, upper part of the vagina and elective lymph nodes [29].

IMPT treatment planning

IMPT treatment plans were generated with RayStation (version 4.4, RaySearch Laboratories AB, Stockholm, Sweden). High-density CT values due to contrast agents used for vagina and bladder visualization were corrected to muscle (1.05 g/cm^3) and water (1.0 g/cm^3) density, respectively. For each patient, three initial IMPT plans based on different fixed beam configurations were created with the beam isocenter set to the GTV center of mass (Table 4.1). The prescribed physical CTV dose of 46 Gy ($23 \times 2 \text{ Gy}$) was planned using a pencil beam scanning technique on a uniform 4 mm dose grid. The planning objectives used for initial IMPT planning consisted of an extended set of planning objectives applied clinically for photon-based RT in order to also penalize intermediate doses to rectum ($V_{30\text{Gy}}$) and bladder ($V_{40\text{Gy}}$) (Table 4.1).

Robust plan optimization

IMPT plans were robustly optimized by minimizing the penalty of the worst-case scenario within the interval of pre-defined range and position errors [129]. Besides the nominal scenario, six position error scenarios were included during optimization by shifting the isocenter position (left, right, inferior, superior, posterior, anterior). In photon-based RT, margins to expand the CTV to form the planning target volume (PTV) are not solely used to correct for geometric uncertainties. However, in this study the clinically used CTV-to-PTV margin in photon-based cervical cancer RT of 8 mm was used as position error for robust optimization. Also, three range error scenarios

were included (-3%, 0%, 3%) per position error scenario [24], resulting in a total of 21 scenarios consisting of both position and range errors considered during optimization.

IMPT plan approval

After robust optimization, IMPT plan quality was first assessed by verifying if the obtained nominal dose distribution fulfilled all pre-defined evaluation objectives (Table 4.1). Next, robustly optimized IMPT plans were evaluated on robustness by applying range and position errors and recalculating the dose. Because robust optimization only included position errors in the main directions, the evaluation on robustness was applied based on an extended set of position errors. Next to the six isocenter position shifts used during optimization (i.e. 8 mm isocenter position shifts in the main directions), eight additional isocenter position shifts of 8 mm along the diagonal of each octant in three-dimensional space were added. Also, minimum (-3%) and maximum (3%) range errors used during optimization were included for evaluation to consider in total 28 perturbed dose scenarios. Robustly optimized IMPT plans were approved when the nominal dose scenario as well as at least 27 out of all 28 perturbed dose scenarios fulfilled all pre-defined evaluation objectives (Table 4.1).

Table 4.1 | Beam configurations with associated gantry angles, initial planning objectives and evaluation objectives used.

Configuration	Gantry angles (°)
2-beam	90, 270
3-beam	0, 90, 270
4-beam	30, 90, 270, 330
Planning objectives	
CTV	Minimum dose 46 Gy ($w=120$) Maximum dose 46.8 Gy ($w=80$; $\sigma=50$)
Body	Dose fall-off: 46–30 Gy over 1.2 cm ($\sigma=0.6$ cm) ($w=50$; $\sigma=30$)
Bladder	Maximum 40 Gy to 20% ($\sigma=10\%$) of the volume ($w=10$; $\sigma=10$)
Rectum	Maximum 30 Gy to 30% ($\sigma=10\%$) of the volume ($w=10$; $\sigma=10$)
Evaluation objectives	
CTV	At least 40 Gy received by 99% of the volume * At most 50.4 Gy received by 2% of the volume
Body	At most 1800 cm ³ receiving 43.7 Gy
Rectum	At most 90% of the volume receiving 30 Gy *
Bowel	At most 600 cm ³ receiving 45 Gy
Bladder	At most 80% of the volume receiving 40 Gy *

Abbreviations: CTV = clinical target volume; w = weight; σ = standard deviation.

Note: Asterisks indicate evaluation objectives used for Pareto front generation.

Pareto front approximation

The scripting facilities in RayStation were used to automatically approximate the Pareto front in robust IMPT planning (Figure 4.1). To start the automatic Pareto front approximation, an initially created IMPT plan with a fixed beam configuration and a set of planning objectives was required and assigned as base plan for the first iteration. Given the IMPT base plan, per iteration multiple IMPT plans were automatically generated with new planning objective values drawn from a Gaussian distribution with the value of the base plan as mean and pre-defined standard deviations. All generated plans were robustly optimized and plan approval was assessed by evaluating the nominal dose scenario as well as the 28 perturbed dose scenarios. When the pre-defined number of IMPT plans per iteration were generated, the dominating plans were derived using all approved IMPT plans from completed iterations. Dominating plans are plans for which one selected evaluation objective for Pareto front generation cannot be improved without deteriorating other selected evaluation objectives for Pareto front generation.

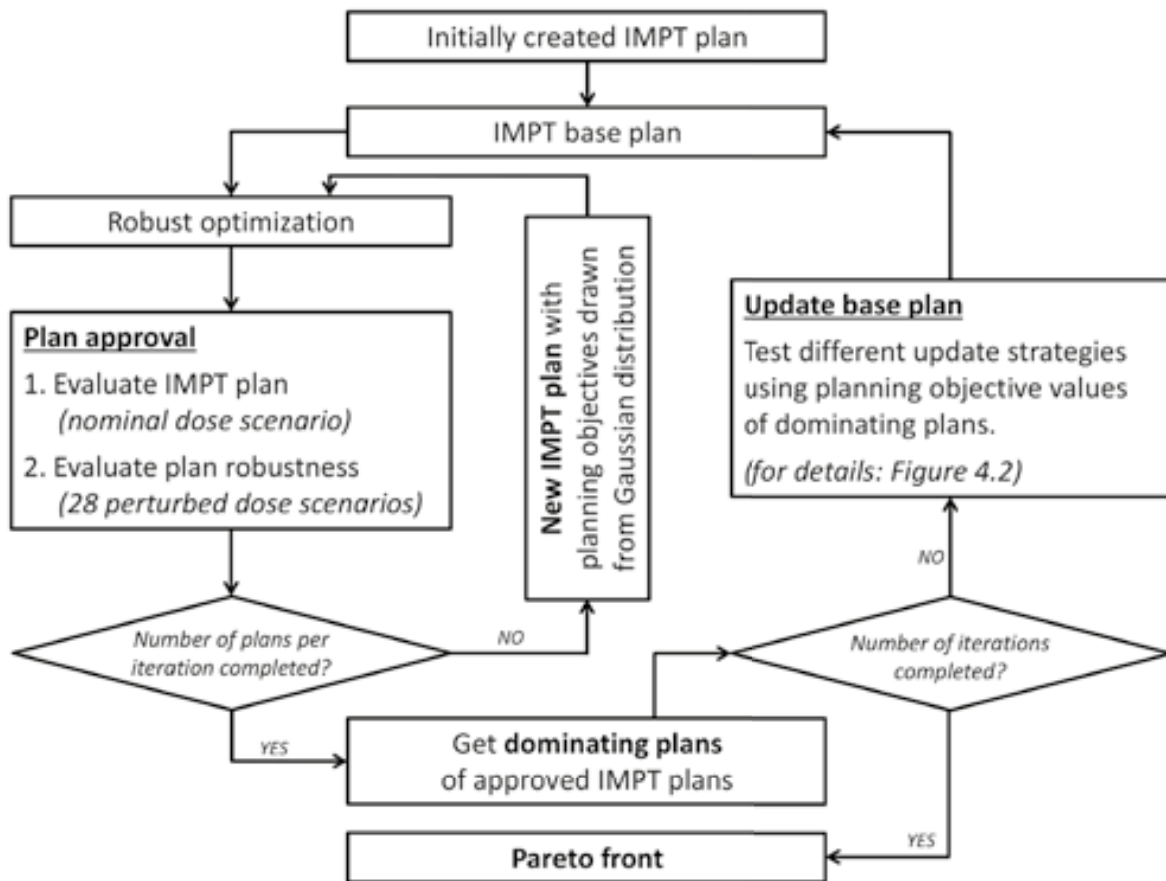


Figure 4.1 | Flowchart of the scripted method to approximate the Pareto front by automatically generating and evaluating multiple IMPT plans, including an update of the base plan after each iteration. The different scenarios tested to update the base plan are illustrated in more detail in Figure 4.2.

A new iteration was started with an updated IMPT base plan to approximate the Pareto front in a more efficient way. To update the base plan, planning objective values of the current base plan were adapted using dominating plans of all completed iterations. For all planning objectives, differences between the value of the current base plan and the average of all dominating plan values (PO_{diff}) were calculated and used to test different update strategies. As a first approach, planning objective values of the current base plan were adapted by subtracting doubled PO_{diff} values and proposed as updated base plan candidate. After robust optimization and assessment of plan approval, this base plan candidate was considered suitable when both the plan was approved and the plan was a dominating plan within the set of approved plans. Alternatively, the described strategy was repeated using 1.5 times PO_{diff} . When both base plan candidates were not suitable, an existing dominating plan close to the current base plan (i.e. minimum sum of squared relative objective differences) was set as updated base plan. Compared to the current base plan, for all strategies the updated base plan should be shifted towards the Pareto front. Figure 4.2 shows a schematic 2D representation of the concept for the different update strategies.

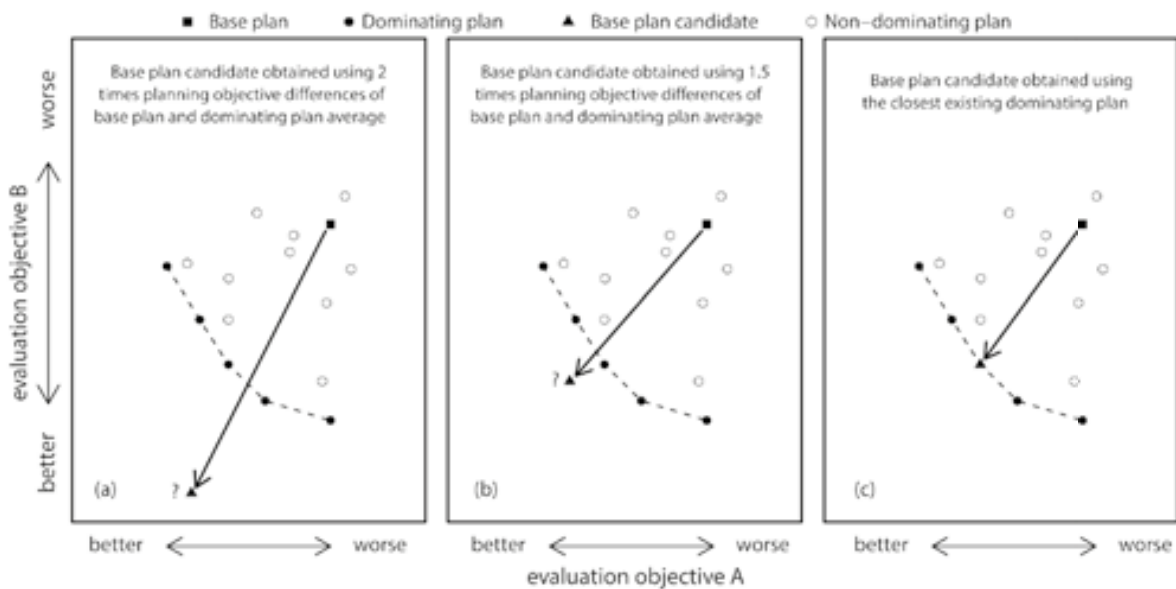


Figure 4.2 | Schematic 2D illustration of the three different strategies tested when updating the base plan. Each example shows the base plan together with approved IMPT plans including the dominating plans for the objectives of interest. First, planning objective value differences between the current base plan and averages of dominating plans were doubled and subtracted from planning objective values of the current base plan (a). This updated base plan candidate is only used when the plan is approved and a dominating plan within the set of generated plans. If strategy A is not suitable, 1.5 times planning objective value differences between the current base plan and averages of dominating plans were subtracted from planning objective values of the current base plan (b). This updated base plan candidate is only used when the plan is approved and a dominating plan within the set of generated plans. When both base plan candidates were not suitable, an existing dominating plan close to the current base plan was set as updated base plan (c).

When the pre-defined number of iterations were completed, the dominating plans of approved IMPT plans from all iterations were derived based on the selected evaluation objectives for Pareto front generation. This derived set of dominating IMPT plans was defined as the Pareto front.

Data analysis

For each included patient, three Pareto fronts corresponding to three pre-defined beam configurations with identical gantry angles were generated. Each Pareto front was approximated using 5 iterations consisting of 40 IMPT plans per iteration. Given all pre-defined evaluation objectives, three evaluation objectives considered clinically most relevant and consistent with planning objectives were selected to span the three-dimensional Pareto front. Table 4.1 presents standard deviations used to automatically generate new planning objective values as well as the subset of evaluation objectives selected for Pareto front generation. The time needed to optimize and approve all IMPT plans on a personal computer with a 8-core, CPU of 2.40 GHz and 48 GB of RAM was recorded.

Per patient and beam configuration, the proportion of non-approved IMPT plans (NA_{IMPT}) was calculated to investigate the effect of beam configuration on plan robustness. Also, from the 200 generated IMPT plans per defined beam configuration the proportion of dominating plans (DP_{IMPT}) that described the Pareto front was assessed. To determine which beam configuration dominates, corresponding Pareto fronts were compared by calculating the proportion of approved IMPT plans contributing to the overall Pareto front. Given sets of approved IMPT plans based on different beam configurations, the overall Pareto front was defined by plans dominating this set of plans.

Differences between Pareto fronts were quantified according to a previously described method [130,131]. For each objective, the distribution of differences was calculated between linearly interpolated surfaces spanned by all other objectives (Figure 4.3). Pareto front differences were represented by the distribution quartiles and only considered appropriate when the overlap between surfaces spanned by all other objectives (i.e. the surface shared by both Pareto fronts divided by the average surface of both Pareto fronts) was at least 10%. This threshold was selected to avoid quantifications based on minimal information without omitting valuable information. Either positive or negative distribution quartiles represented overall differences between Pareto fronts (i.e. one Pareto front is dominated by the other Pareto front) while both positive and negative distribution quartiles indicated a Pareto front crossing.

When a limited or no overlap was observed between linearly interpolated surfaces, the proposed method could not be performed and an alternative method to compare Pareto fronts was used (Figure 4.3). Without keeping all other objectives constant, objective differences between individual dominating plans of both Pareto fronts were determined. Based on the derived distribution of differences, Pareto front ranges for the given objective were compared without taking into account all other objectives. Objective ranges were considered similar when the interval

defined by the first and third distribution quartile (I_{Q1-Q3}) contained both positive and negative difference values. A complete positive or negative interval represented a substantial objective range difference between Pareto fronts.

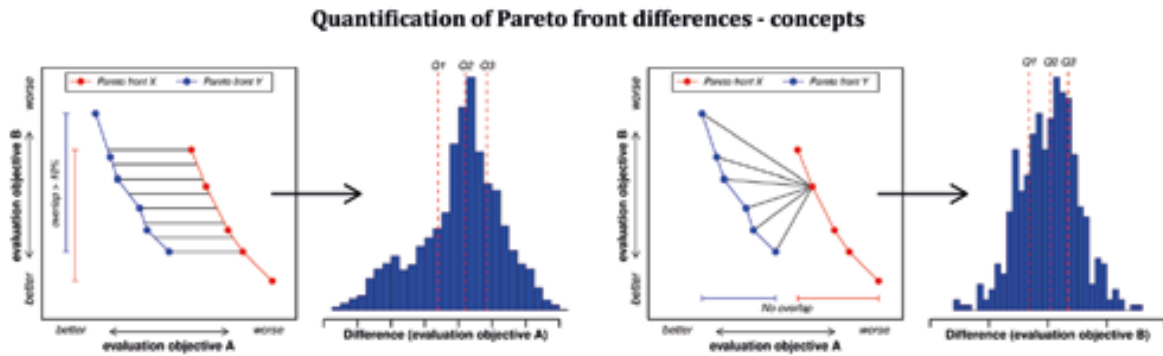


Figure 4.3 | A 2D representation of the concepts to quantify the differences between Pareto fronts. The figure on the left side illustrates the quantification of Pareto front differences for evaluation objective A. Since the overlap between surfaces spanned by all other evaluation objectives (e.g. evaluation objective B) is substantial (>10%), the distribution of differences and associated quartiles between the linearly interpolated surfaces were calculated. The figure on the right side illustrates the quantification of Pareto front differences for evaluation objective B. Since no overlap between surfaces spanned by all other evaluation objectives (e.g. evaluation objective A) is observed, evaluation objective differences between dominating IMPT plans were calculated. Based on the interval defined by associated distribution quartiles, evaluation objective ranges were compared.

4.3 | Results

For each patient and pre-defined beam configuration, three-dimensional Pareto fronts were successfully sampled based on 200 IMPT plans. On average, robust optimization and consecutively plan approval of one IMPT plan took 40 minutes, 55 minutes and 75 minutes for the 2-beam, 3-beam and 4-beam set-up, respectively. As an example, Figure 4.4 shows a two-dimensional representation of the derived three-dimensional Pareto fronts of robust IMPT plans for one arbitrarily selected patient. Derived Pareto fronts of all patients can be found in the supplementary data available online¹. In addition, an example representing dose distributions of dominating plans for the different beam configurations is shown (Figure 4.5).

Given all robustly optimized IMPT plans, the average proportion of non-approved IMPT plans was 32% (range, 12%–41%), 29% (range, 12%–43%) and 28% (range, 19%–45%) for the configuration using two beams, three beams and four beams, respectively. In all patients, IMPT plans based on the 2-beam set-up were completely dominated by plans with other beam configurations.

¹ stacks.iop.org/PMB/61/1780/mmedia

For the 3-beam and 4-beam set-up, the average proportion of dominating plans contributing to the overall front was 28% (range, 12%–45%) and 72% (range, 55%–88%), respectively. Table 4.2 summarizes patient-specific proportions of NA_{IMPT} and DP_{IMPT} together with patient-specific proportions of dominating plans contributing to the overall Pareto front.

Table 4.2 | Percentages of non-approved IMPT plans (NA_{IMPT}) and dominating IMPT plans (DP_{IMPT}) as well as percentages of dominating plans contributing to the overall patient-specific Pareto surface based on all approved IMPT plans per patient.

Patient	NA_{IMPT} (DP_{IMPT})			Overall Pareto front		
	2B	3B	4B	2B	3B	4B
1	38.0 (19.0)	11.7 (18.0)	22.9 (20.5)	0.0	12.5	87.5
2	40.5 (16.0)	29.5 (30.5)	33.0 (28.0)	0.0	21.7	78.3
3	30.5 (16.0)	39.5 (13.0)	21.5 (22.5)	0.0	24.5	75.5
4	40.0 (20.5)	43.0 (19.5)	45.0 (13.5)	0.0	45.5	54.5
5	12.0 (17.5)	23.5 (18.0)	18.5 (12.5)	0.0	33.3	66.7
Average	32.2 (17.8)	29.4 (19.8)	28.2 (19.4)	0.0	27.5	72.5

Abbreviations: 2B = 2-beam set-up; 3B = 3-beam set-up; 4B = 4-beam set-up.

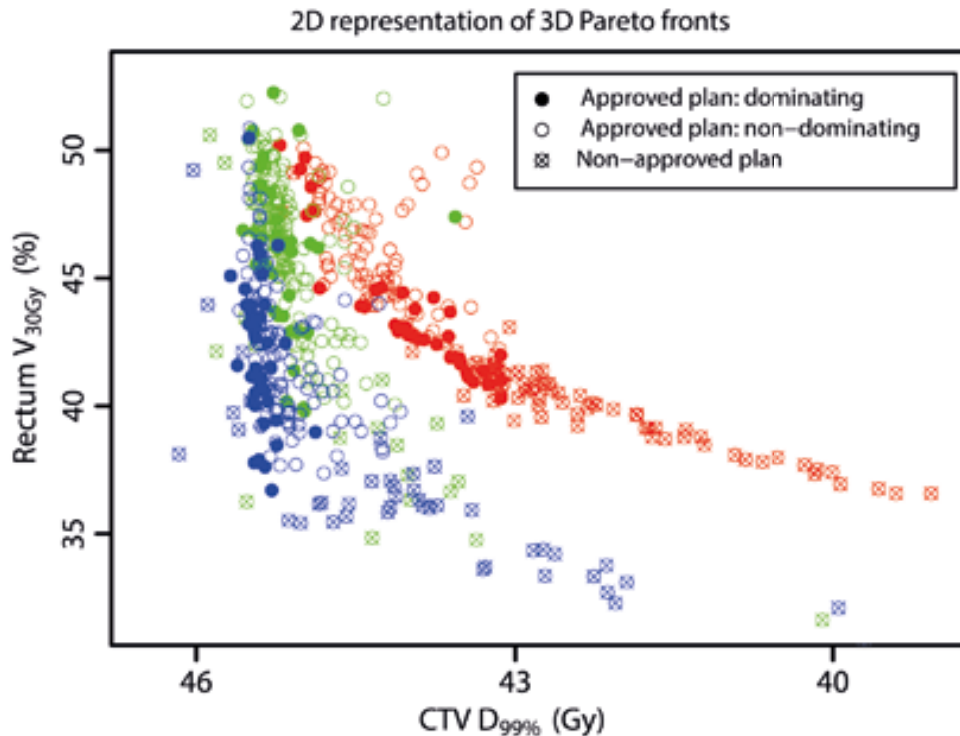


Figure 4.4 | 2D representation of 3D Pareto fronts sampled using 200 generated IMPT plans and the nominal dose distribution is represented by dots for beam configurations using 2 beams (red), 3 beams (green) and 4 beams (blue). Per beam configuration, dominating plans are presented by filled dots and non-approved plans are represented by crossed dots.

Table 4.3 | Results of the quantified differences between Pareto fronts per patient. For each evaluation objective, the quartiles of the difference distribution are presented. If no difference distribution could be determined while keeping all other objectives constant (indicated by a cross), results of the comparison between evaluation objective ranges and associated intervals (I_{Q1-Q3}) are presented. Interpretation of results: Pareto front based on the first beam set-up compared to the Pareto front based on the second beam set-up (second column).

Patient	CTVD _{99%} (Gy)		Rectum V _{30Gy} (%)		Bladder V _{40Gy} (%)		
	Q2 (Q1 - Q3)	objective range; (I_{Q1-Q3})	Q2 (Q1 - Q3)	objective range; (I_{Q1-Q3})	Q2 (Q1 - Q3)	objective range; (I_{Q1-Q3})	
1 3B-2B	x	difference; (0.7-1.7)	x	similar; (-0.5-5.1)	-13.5 (-11.8- -14.8)	x	difference; (-12.7- -8.1)
4B-2B	x	difference; (1.0-1.8)	x	similar; (-4.1-0.8)			
4B-3B	0.3 (0.2-0.3)		-6.5 (-7.8- -5.0)		-4.1 (-5.2- -2.9)		
2 3B-2B	1.4 (1.0-1.7)		-12.2 (-13.6- -10.4)		-10.3 (-12.4- -8.9)		
4B-2B	x	difference; (0.2-1.3)	x	difference; (-17.1- -9.2)	x		difference; (-7.1- -0.9)
4B-3B	0.3 (0.1-0.5)		-5.9 (-8.2- -4.1)		-0.6 (-1.7-0.5)		
3 3B-2B	0.7 (0.6-0.8)		x	similar; (-7.5-0.1)	-7.8 (-8.6- -5.6)		
4B-2B	0.5 (0.4-0.7)		-1.4 (-3.1-0.1)		-8.3 (-10.2- -6.3)		
4B-3B	0.1 (0.0-0.1)		-2.4 (-5.5- -0.1)		-0.4 (-1.7-0.6)		
4 3B-2B	1.6 (1.3-1.8)		-11.1 (-12.0- -9.3)		-11.2 (-11.9- -10.3)		
4B-2B	1.8 (1.7-1.8)		x	difference; (-7.8- -0.4)	x		difference; (-7.6- -2.5)
4B-3B	0.1 (-0.1-0.3)		-1.4 (-2.4- -0.3)		-0.8 (-1.6- -0.1)		
5 3B-2B	0.5 (0.4-0.6)		x	difference; (-6.1- -2.1)	-3.2 (-3.5- -2.8)		
4B-2B	0.5 (0.4-0.6)		x	difference; (-7.5- -2.6)	x		similar; (-1.5-1.0)
4B-3B	0.1 (0.1-0.2)		-1.8 (-3.0- -0.7)		-0.7 (-1.1- -0.3)		

Abbreviations: Q1 = first quartile; Q2 = second quartile; Q3 = third quartile; 2B = 2-beam set-up; 3B = 3-beam set-up; 4B = 4-beam set-up.

Differences between Pareto fronts based on the 3-beam and 4-beam set-up in one objective were quantified for all patients using the surface spanned by the other two objectives. Compared to the 3-beam configuration, the median CTV $D_{99\%}$ increased on average by 0.2 Gy when using the 4-beam configuration and the median rectum $V_{30\text{Gy}}$ and bladder $V_{40\text{Gy}}$ decreased on average by 3.6% and 1.3%, respectively. For the Pareto fronts based on the 2-beam configuration, differences with other Pareto fronts were quantified using the surface spanned by the other two objectives or individual dominating plans. Compared to the 2-beam configuration, evaluation objective range differences with positive interval values indicated improvements in CTV $D_{99\%}$ for the 3-beam and 4-beam configuration, respectively. For both rectum $V_{30\text{Gy}}$ and bladder $V_{40\text{Gy}}$, the 3-beam configuration as well as the 4-beam configuration resulted in similar or improved objective ranges. Table 4.3 summarizes the results of comparisons between obtained Pareto fronts for different beam configurations per patient.

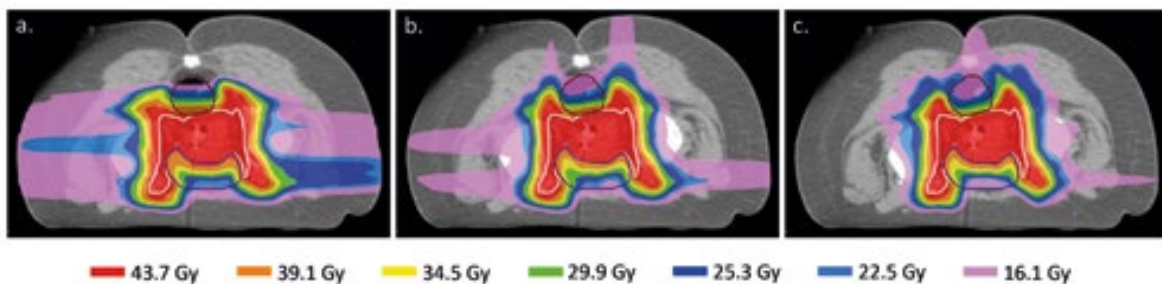


Figure 4.5 | For one patient, color wash map examples of dose distributions corresponding to dominating plans are shown for the 2-beam (a), 3-beam (b) and 4-beam (c) configuration. All dose distributions indicated adequate CTV (white) coverage while differences in dose to rectum (brown) and bladder (purple) are observed.

4.4 | Discussion

We implemented a method to automatically approach the Pareto front of robust IMPT plans to enable beam configuration selection for cervical cancer PT. By comparing clinically relevant Pareto fronts of robust IMPT plans for different gantry angle sets, the most favourable beam configuration in terms of inspected parameters was selected. The presented study was the first to investigate the effect of beam configurations on robust IMPT planning, which included robust optimization followed by an evaluation of the actual robustness, and to compare Pareto fronts for beam configuration selection. A total of 200 robust IMPT plans per beam configuration per patient resulted in configuration-specific Pareto fronts, allowing us to objectively compare the effect of different beam set-ups on plan quality for beam configuration selection in cervical cancer PT. Our study showed that per beam configuration a substantial part of the robustly optimized IMPT plans (i.e. on average 29%) was not approved after robustness evaluation. For all patients, the defined

configuration using two beams was inferior compared to the other specified beam configurations in terms of robustness, target coverage and OARs sparing. Although differences with the specified 3-beam set-up are small, IMPT plans based on the defined 4-beam set-up largely dominated the overall Pareto fronts.

Unlike beam configurations used in previous studies on proton-based cervical cancer RT [70,71,123,124], we demonstrated the feasibility of beam configuration selection in cervical cancer PT by objectively comparing Pareto fronts based on different gantry angle sets. The optimal exploitation of proton therapy for specific tumor sites (e.g. cervical cancer) will only be achieved by determining the optimal beam configuration. Moreover, range and position uncertainties can largely affect IMPT dose distributions [122,132]. However, the effect of uncertainties on dose delivery in proton-based cervical cancer RT is not yet investigated. Together with the lack of beam configuration comparisons in cervical cancer, previously reported results on proton-based RT for cervical cancer might need to be interpreted with caution.

Even though the feasibility of using Pareto fronts as a comparative tool for treatment strategies and delivery techniques was proven [128], only a limited number of studies reported on the use of Pareto fronts for treatment technique comparison or treatment plan validation [130,131,133]. Along the lines of these studies, we implemented our method to automatically approach the Pareto front in robust IMPT planning. Besides the addition of robustness validation after robust optimization, we also added the efficiency of approaching the Pareto front by starting each iteration with an updated base plan [134].

Instead of Pareto front approximation based on random sampling used in this study, Pareto fronts could theoretically also be approached by using mathematically derived gradient directions to approximate towards the Pareto front [135]. However, for relatively simple multi-criteria optimization problems already a complex situation arises and implementation of this mathematical method is beyond the clinical purpose of our study.

In this study, we compared three pre-defined beam configurations for PT in the pelvic region using three-dimensional Pareto fronts based on robust IMPT planning. The pre-defined beam set-ups consisted of a limited number of beams, resulting in relatively short delivery times and limited inter-beam patient movement errors. Combined with the defined update strategy, three-dimensional Pareto fronts are approximated using a relatively large number of IMPT plans and therefore assumed to represent realistic trade-offs between target coverage and OAR sparing. Although three-dimensional Pareto fronts were sampled in this study based on the subset of evaluation objectives selected for Pareto front generation, the presented method can be used to sample and compare multidimensional Pareto fronts based on multiple selected evaluation objectives. However, an increased number of evaluation objectives used for Pareto front generation requires a larger number of IMPT plans to sufficiently sample multidimensional Pareto fronts.

Although the application of planning objectives used clinically for photon-based RT, initial IMPT treatment plans resulted already in relatively good IMPT plans. Therefore, only a limited number of iterations were needed to sample the clinically most relevant parts of the Pareto front.

However, the use of these initial plans also steered already towards specific parts of the Pareto front and approximated Pareto fronts could therefore not always be compared quantitatively. If the current calculation times can be largely reduced, sufficiently sampling the entire Pareto front by using multiple starting positions could solve this issue.

In this study, sets of dominating IMPT plans acquired with identical optimization conditions were compared and spot filtering using the machine-specific minimum monitor units (MU) was not included in the IMPT optimization process. However, the influence of spot filtering using the machine-specific MU minimum on optimized dose distributions was investigated. Because the contribution of spots with below minimum MU was expected to increase with the number of beams, a subset of dominating plans based on the 4-beam configuration was also optimized including spot filtering. The minor differences (<2%) found between dose distributions obtained with and without spot filtering indicated reliable results presented in this study.

For robust optimization and evaluation on robustness, the range error value was selected based on literature [24] and the clinically used CTV-to-PTV margin in photon-based RT for cervical cancer was used to define the position error. These values directly determine IMPT plan robustness, but whether the selected values are adequate to anticipate on patient-specific uncertainties during the course of treatment can only be validated using daily imaging. Although all plans were robustly optimized, on average 29% was not approved after evaluation using the same error values. Nevertheless, the error values were considered adequate and for the purpose of this study were kept constant to reliably compare Pareto fronts based on different beam configurations. Additional research is required to quantify individual error values and corresponding consequences for dose distributions obtained with specific beam configurations.

Compared to analytical dose calculation algorithms, a Monte Carlo algorithm might improve the accuracy of dose calculation in complex geometries [136]. In the pelvic area, as in this study, effects of inhomogeneities mainly due to air and bone are limited and dose distributions can be calculated accurately using an analytical algorithm. Therefore, the limitation induced by the dose calculation algorithm was assumed to be negligible.

Because of a limited overlap, the quantification of Pareto front differences based on linearly interpolated surfaces could not be performed for all objectives. The overlap threshold of 10% was selected to avoid quantifications based on minimal information while an increase of this threshold could omit valuable information. Although Pareto fronts with a limited overlap could also be extrapolated to enable quantification, Pareto front differences would strongly depend on only a few IMPT plans without representing realistic differences. As an alternative, differences between individual dominating plans were calculated without keeping all other objectives constant.

Although the limited number of patients included in this study, all patients showed similar results with respect to the optimal beam configuration in terms of DVH parameters. However, general conclusions on beam configuration selection in cervical cancer PT can only be drawn when more patients are included. Since the calculation time is the limiting factor, for one patient we explored the possible reduction in calculation time by using RayStation version 4.6.102.4 installed

on a personal computer with 2 CPUs of 12 physical cores each. The average calculation time reduction of 70% found for this patient opens the possibility to extend this study in future.

Besides the approximation of Pareto fronts based on robust IMPT planning in cervical cancer, our presented method to approach the Pareto front is generic and therefore can be applied for different treatment sites. Although our strategy is especially developed for proton-based RT by focusing on plan robustness, also Pareto fronts of photon-based plans can be derived to improve clinically obtained RT plans or compare RT treatment techniques.

To actually take advantage of the planned IMPT dose distributions acquired with the selected beam configuration, anticipation on interfraction anatomical changes during fractionated EBRT in cervical cancer is required. Pre-fraction imaging allows, besides verifying the patient position accurately, adapting the radiation delivery during the treatment course and automatic segmentation tools are developed to support these purposes [75,76]. Nevertheless, the dosimetric advantages of proton therapy compared with photon therapy for cervical cancer patients using the selected beam configuration combined with an adaptive strategy to compensate for interfraction anatomical changes are being investigated.

4.5 | Conclusion

This study demonstrated a method to automatically approach the Pareto front in robust IMPT treatment planning. For five cervical cancer patients, we derived and compared Pareto fronts based on robust IMPT plans for three different beam configurations. For all patients, the defined 4-beam configuration was found to be optimal in terms of robustness, target coverage and OAR sparing.